Supplementary Figures

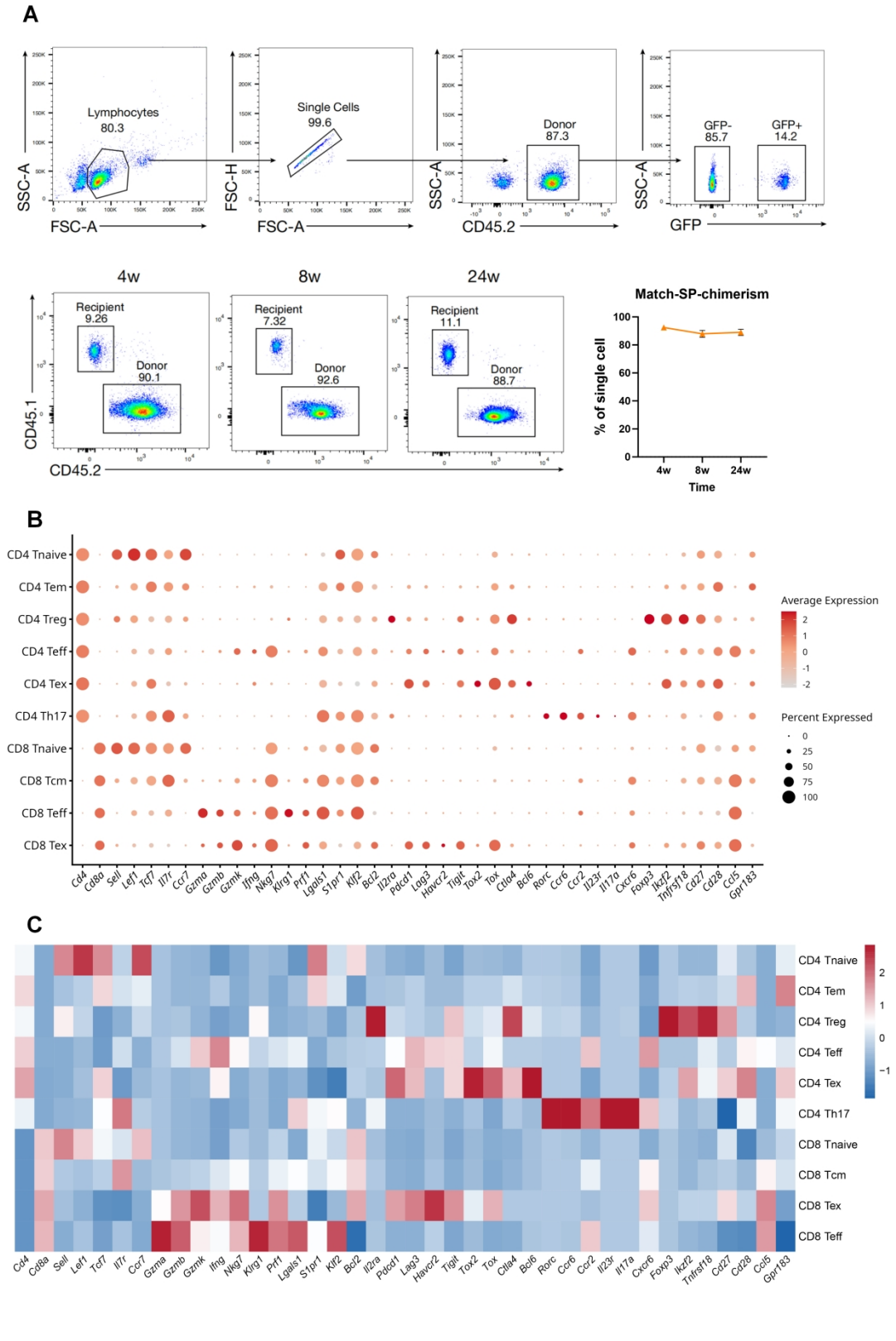

Figure S1. Gating strategy for splenic transplant chimerism analysis and marker-based validation of CD4$^+$ and CD8$^+$ T-cell subset identity.

(A) Representative flow cytometric gating strategy used to assess donor chimerism in splenocytes from the matched transplantation model. Representative plots show recipient (CD45.1$^+$) versus donor (CD45.2$^+$) chimerism among splenic single cells at 4, 8, and 24 weeks post-transplantation. Right, donor chimerism (% of single cells) over time (mean ± SEM; n = 3 mice per time point).

(B, C) Marker-based validation of the cluster annotations shown in Figure 1b. Dot plot (B) and heatmap (C) showing expression of canonical lineage and functional markers, validating the cluster annotations used throughout this study.

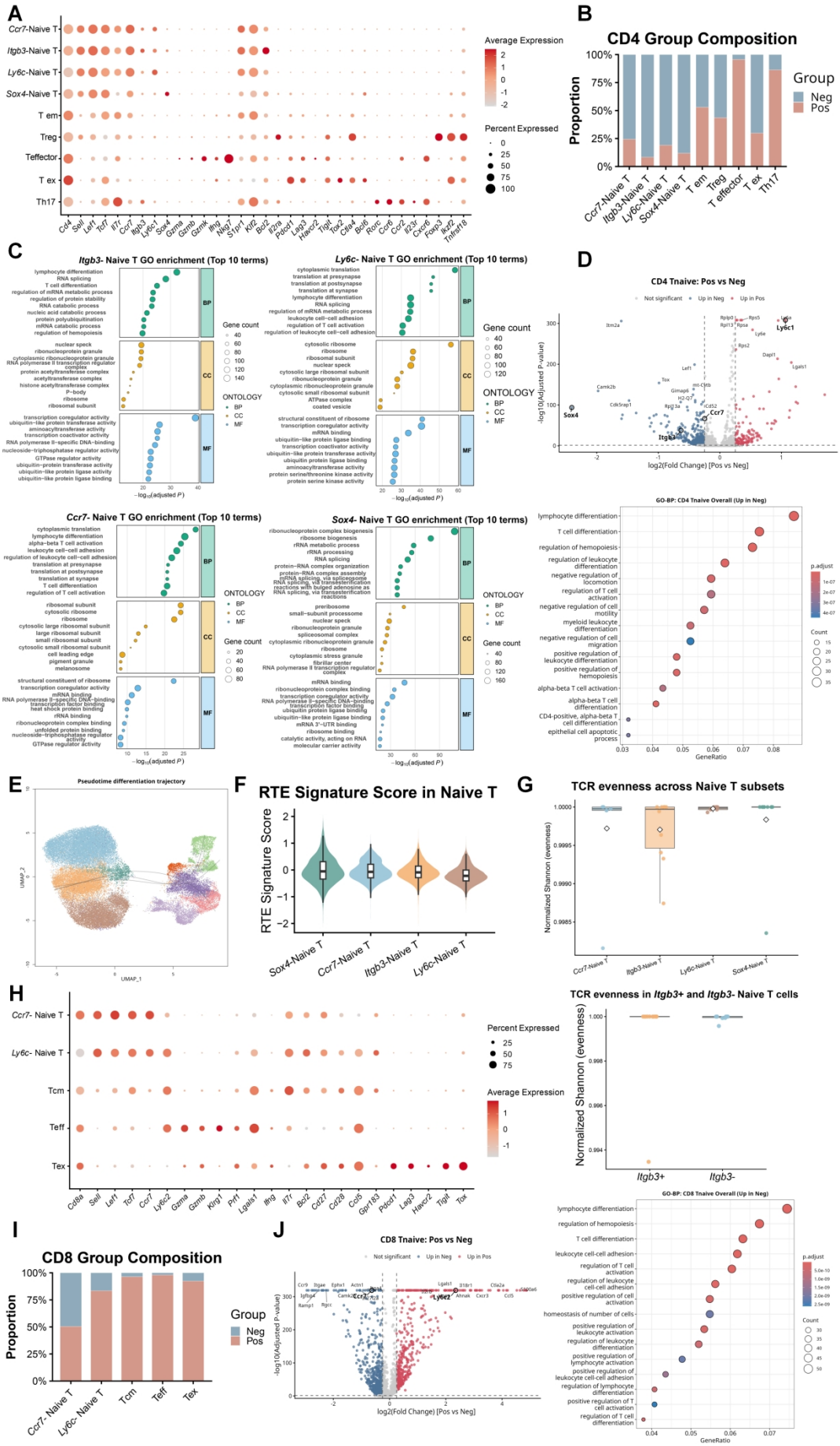
A
Ccr7-Naive T
Itgb3-Naive T
Ly6c-Naive T
Sox4-Naive T
T em
Treg
Teffector
T ex
Th17
Average Expression
Percent Expressed
B
CD4 Group Composition
Proportion
Group
Neg
Pos
C
Itgb3- Naive T GO enrichment (Top 10 terms)
Ly6c- Naive T GO enrichment (Top 10 terms)
Ccr7- Naive T GO enrichment (Top 10 terms)
Sox4- Naive T GO enrichment (Top 10 terms)
BP
CC
MF
Gene count
ONTOLOGY
D
CD4 Tnaive: Pos vs Neg
Not significant
Up in Neg
Up in Pos
log2(Fold Change) [Pos vs Neg]
GO-BP: CD4 Tnaive Overall (Up in Neg)
GeneRatio
p.adjust
Count
E
Pseudotime differentiation trajectory
F
RTE Signature Score in Naive T
RTE Signature Score
G
TCR evenness across Naive T subsets
Normalized Shannon (evenness)
H
Tcm
Teff
Tex
TCR evenness in Itgb3+ and Itgb3- Naive T cells
Itgb3+
Itgb3-
I
CD8 Group Composition
J
CD8 Tnaive: Pos vs Neg
GO-BP: CD8 Tnaive Overall (Up in Neg)

Figure S2. Marker-based validation, functional annotation, and TCR repertoire analysis of naïve T-cell subsets.

(A) Dot plot of subset-defining and canonical T-cell markers across CD4+ clusters (Ccr7-, Itgb3-, Ly6c-, Sox4-naïve T, Tem, Treg, Teffector, Tex, Th17), validating cluster annotation.

(B) Proportion of GFP^- (Neg) and GFP^+ (Pos) cells within each $CD4^+$cluster.

(C) Top 10 GO terms (Biological Process, Cellular Component, Molecular Function) enriched among genes upregulated in each $CD4^+$ naïve subset (*Itgb3*-, *Ly6c*-, *Ccr7*-, *Sox4*-naïve T) relative to the other three.

(D) Volcano plot (top) and GO-BP enrichment (bottom) comparing GFP^+ (Pos) versus GFP^- (Neg) $CD4^+$ naïve T cells overall.

(E) Pseudotime differentiation trajectory of $CD4^+$ naïve T-cell subsets.

(F) RTE signature score across the four $CD4^+$ naïve subsets, note that the signature includes *Sox4* and *Pecam1*, which also define individual subsets, limiting the discriminative power of this composite score among closely related subsets.

(G) TCR repertoire evenness (normalized Shannon index) across the four $CD4^+$ naïve subsets (top) and between $Itgb3^+$ and $Itgb3^-$ $CD4^+$ naïve T cells (bottom).

(H) Dot plot of marker gene expression across $CD8^+$ clusters (*Ccr7*-, *Ly6*c-naïve T, Tcm, Teff, Tex) (left) and TCR evenness between *Itgb3*+ and *Itgb3*- $CD8^+$ naïve T cells (right).

(I) Proportion of GFP^- and GFP^+ cells within each $CD8^+$ cluster.

(J) Volcano plot (left) and GO-BP enrichment (right) comparing GFP^+ versus GFP^- $CD8^+$ naïve T cells overall.

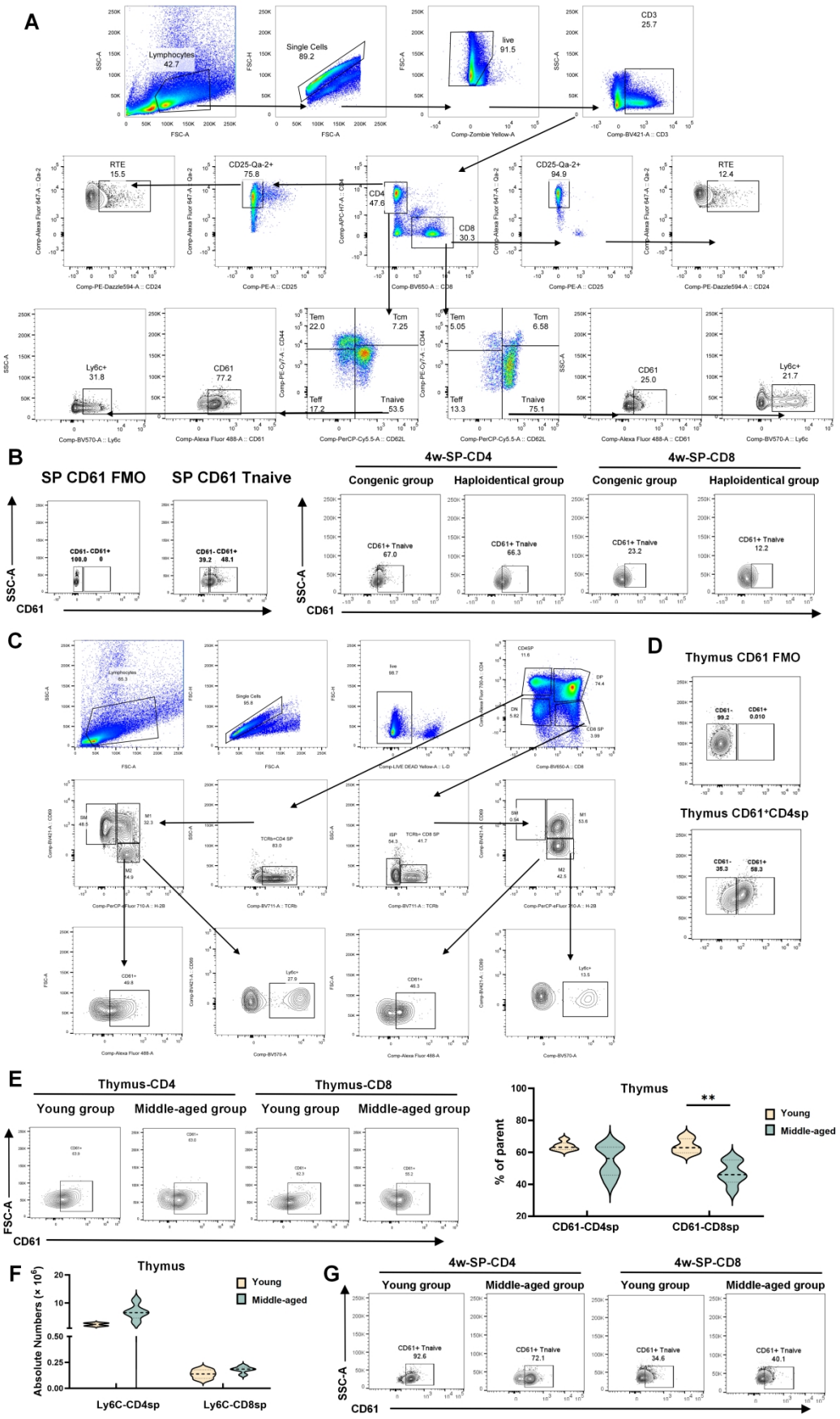
A
Lymphocytes
42.7
Single Cells
89.2
live
91.5
CD3
25.7
RTE
15.5
CD25-Qa-2+
75.8
CD4
47.6
CD8
30.3
CD25-Qa-2+
94.9
RTE
12.4
Ly6c+
31.8
CD61
77.2
Tem
22.0
Tcm
7.25
Teff
17.2
Tnaive
53.5
Tem
5.05
Tcm
6.58
Teff
13.3
Tnaive
75.1
CD61
25.0
Ly6c+
21.7
B
SP CD61 FMO
SP CD61 Tnaive
4w-SP-CD4
Congenic group
Haploidentical group
4w-SP-CD8
Congenic group
Haploidentical group
CD61+ Tnaive
67.0
CD61+ Tnaive
66.3
CD61+ Tnaive
23.2
CD61+ Tnaive
12.2
SSC-A
CD61
C
D
Thymus CD61 FMO
Thymus CD61+CD4sp
E
Thymus-CD4
Thymus-CD8
Young group
Middle-aged group
Young group
Middle-aged group
Thymus
**
Young
Middle-aged
% of parent
CD61-CD4sp
CD61-CD8sp
F
Thymus
Young
Middle-aged
Absolute Numbers (× 10⁶)
Ly6C-CD4sp
Ly6C-CD8sp
G
4w-SP-CD4
4w-SP-CD8
Young group
Middle-aged group
Young group
Middle-aged group
CD61+ Tnaive
92.6
CD61+ Tnaive
72.1
CD61+ Tnaive
34.6
CD61+ Tnaive
40.1

Figure S3. Gating strategies and CD61 FMO controls for splenic and thymic flow cytometry.

(A) Representative gating strategy for splenic T cells: lymphocytes → single cells → live cells → $CD3^+$ → $CD4^+$/$CD8^+$ → RTE ($CD24^+Qa\text{-}2^+$) and non-RTE ($CD25^-Qa\text{-}2^+$) fractions → naïve ($CD44^-CD62L^+$), Tcm, Tem, and Teff subsets within $CD4^+$ and $CD8^+$ compartments, followed by $Ly6C^+$ and $CD61^+$ gating within naïve T cells.

(B) CD61 gating in splenic $CD4^+$ and $CD8^+$ naïve T cells. Left, CD61 FMO control and corresponding fully stained naïve T-cell sample. Right, representative $CD61^+$ naïve T-cell gating in congenic and haploidentical recipients at 4 weeks post-transplantation, corresponding to Figure 3b.

(C) Representative gating strategy for thymocytes: lymphocytes → single cells → live cells → CD4/CD8 double-positive (DP) and single-positive (SP) populations → TCRβ-defined DP subsets → $CD69^+$ and mature SP populations, followed by $CD61^+$ and $Ly6C^+$ gating within CD4SP and CD8SP thymocytes.

(D) CD61 FMO control (top) and corresponding $CD61^+$CD4SP gating (bottom) in the thymus.

(E) Representative CD61 gating (left) and quantification of CD61-CD4SP and $CD61^-$CD8SP thymocytes as a percentage of parent population (right) in young and middle-aged mice (mean ± SEM; $^{**}p < 0.01$, two-tailed unpaired t-test).

(F) Absolute numbers of Ly6C-CD4SP and Ly6C-CD8SP thymocytes in young and middle-aged mice.

(G) Representative $CD61^+$ naïve T-cell gating in splenic $CD4^+$ and $CD8^+$ compartments from young and middle-aged mice, corresponding to Figure 3e.

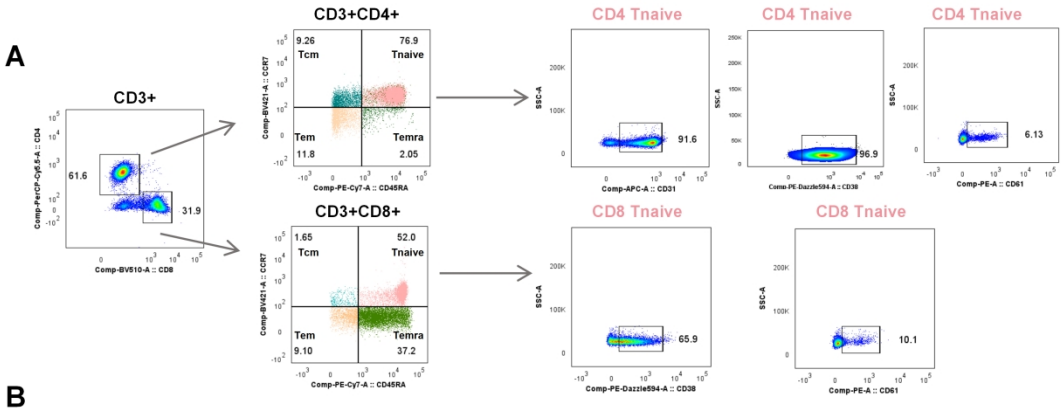
A
CD3+
CD3+CD4+
CD3+CD8+
CD4 Tnaive
CD4 Tnaive
CD4 Tnaive
CD8 Tnaive
CD8 Tnaive
9.26
Tcm
76.9
Tnaive
Tem
11.8
Temra
2.05
1.65
Tcm
52.0
Tnaive
Tem
9.10
Temra
37.2
61.6
31.9
91.6
96.9
6.13
65.9
10.1

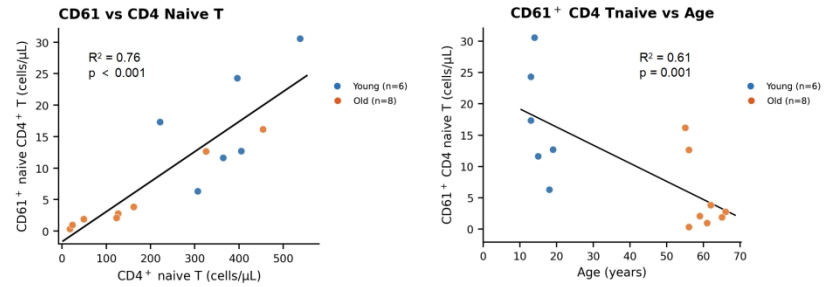
B
CD61 vs CD4 Naive T
R² = 0.76
p < 0.001
CD61⁺ naive CD4⁺ T (cells/μL)
CD4⁺ naive T (cells/μL)
Young (n=6)
Old (n=8)
CD61⁺ CD4 Tnaive vs Age
R² = 0.61
p = 0.001
CD61⁺ CD4 naive T (cells/μL)
Age (years)

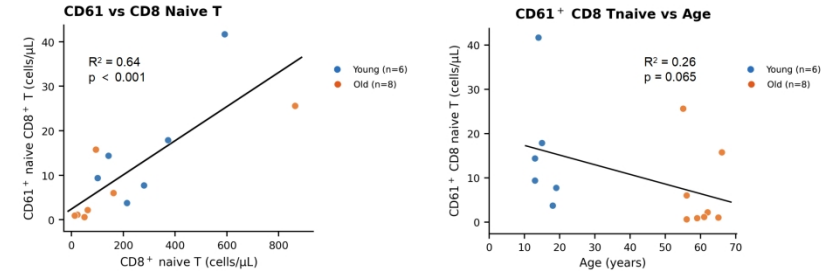
C
CD61 vs CD8 Naive T
R² = 0.64
p < 0.001
CD61⁺ naive CD8⁺ T (cells/μL)
CD8⁺ naive T (cells/μL)
Young (n=6)
Old (n=8)
CD61⁺ CD8 Tnaive vs Age
R² = 0.26
p = 0.065
CD61⁺ CD8 naive T (cells/μL)
Age (years)

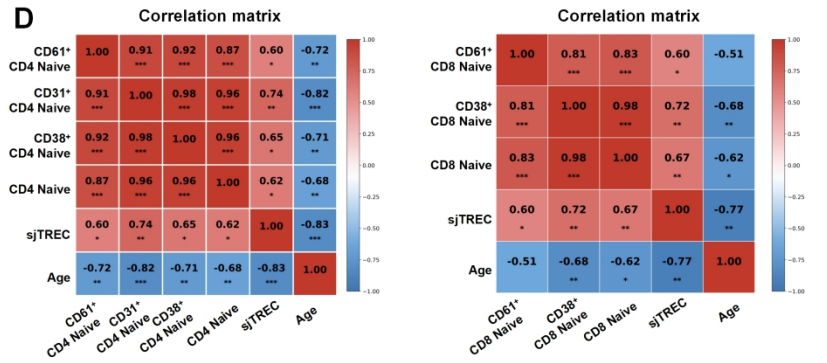
D
Correlation matrix
CD61⁺ CD4 Naive
CD31⁺ CD4 Naive
CD38⁺ CD4 Naive
CD4 Naive
sjTREC
Age
Correlation matrix
CD61⁺ CD8 Naive
CD38⁺ CD8 Naive
CD8 Naive
sjTREC
Age

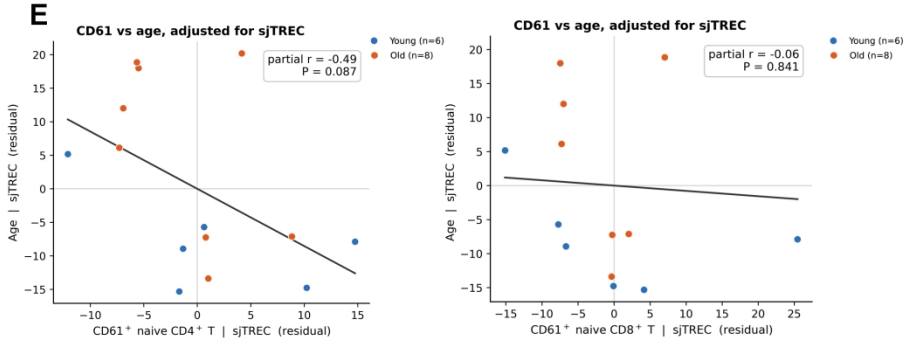
E
CD61 vs age, adjusted for sjTREC
partial r = -0.49
P = 0.087
Age | sjTREC (residual)
CD61⁺ naive CD4⁺ T | sjTREC (residual)
Young (n=6)
Old (n=8)
CD61 vs age, adjusted for sjTREC
partial r = -0.06
P = 0.841
Age | sjTREC (residual)
CD61⁺ naive CD8⁺ T | sjTREC (residual)

Figure S4. Human PBMC flow cytometric gating, CD61 correlation, and partial correlation analyses.

(A) Representative gating strategy for $CD4^+$ and $CD8^+$ naïve T cells ($CCR7^+CD45RA^+$) in human PBMCs, followed by $CD31^+$, $CD38^+$, and $CD61^+$ gating within each naïve subset.

(B, C) Pearson correlation between $CD61^+$ naïve T-cell counts and total naïve T-cell counts (left) and between $CD61^+$ naïve T-cell counts and age (right), for $CD4^+$ (B) and $CD8^+$ (C) compartments. Young (n = 6) and old (n = 8) donors are shown in blue and orange, respectively. R^2 and P values from Pearson correlation are indicated.

(D) Correlation matrices showing pairwise Pearson correlation coefficients among $CD61^+$, $CD31^+$, and $CD38^+$ naïve T-cell counts, total naïve T-cell counts, sjTREC levels, and age, for $CD4^+$ (left) and $CD8^+$ (right) naïve T cells (*p < 0.05, **p < 0.01, ***p < 0.001).

(E) Partial correlation between $CD61^+$ naïve T-cell counts and age, controlling for sjTREC levels, for $CD4^+$ (left) and $CD8^+$ (right) naïve T cells. Axes show residuals after regressing each variable on sjTREC. Partial correlation coefficients and P values are indicated.